Regenerative Therapy 24 (2023) 426–433

Contents lists available at ScienceDirect

Regenerative Therapy

journal homepage: http://www.elsevier.com/locate/reth

Original Article

Lung regeneration with rat fetal lung implantation and promotion of alveolar stem cell differentiation by corticosteroids

Daisuke Matsumoto [a], Hiroaki Toba [a, *], Koichiro Kenzaki [b], Shoji Sakiyama [c], Shinichi Sakamoto [a], Mika Takashima [a], Naoya Kawakita [a], Hiromitsu Takizawa [a]

[a] Department of Thoracic and Endocrine Surgery and Oncology, Institute of Biomedical Sciences, The University of Tokushima Graduate School, Tokushima, Japan
[b] Department of Thoracic and Breast Surgery, Takamatsu Red Cross Hospital, Takamatsu, Japan
[c] Department of Thoracic Surgery, National Hospital Organization Kochi National Hospital, Kochi, Japan

ARTICLE INFO

Article history:
Received 21 May 2023
Received in revised form
21 August 2023
Accepted 7 September 2023

Keywords:
Lung regeneration
Implantation
Fetal lung tissue
Corticosteroids
Alveolar stem cells
microRNA

ABSTRACT

Introduction: The lung is a difficult organ to regenerate, and the development of functional lungs has still not been achieved. In this study, we investigated lung regeneration using a rat fetal lung tissue-implanted model. This study aimed to evaluate the functioning of the implanted fetal lung tissue and investigate the graft differentiation and maturation mechanism, focusing on alveolar stem cells.
Methods: Fetal lung tissue fragments were obtained from Lewis rats on day 17 and implanted into adult lungs. Animals were divided into the following three groups: group 1, injection into the adult left lung parenchyma; group 2, injection with post-caval lobectomy; and group 3, injection with post-caval lobectomy and corticosteroid administration. Computed tomography was performed on weeks 1, 2, 4, and 8. The presence of alveolar pore, CD31 expression, and bipotential progenitor cell (podoplanin+/surfactant protein C+) localization were histologically evaluated. MiRNA expression was comprehensively compared among the three groups.
Results: The grafts comprised type I and type II alveolar cells connected to the recipient lungs with alveolar pores and capillary networks in the interstitial tissue. The alveolar space was the largest and the computed tomography value was the lowest in the grafts of the corticosteroid-administered group. The number of bipotential progenitor cells was the lowest in the corticosteroid administration group on day 7. Moreover, microRNA-487-3p, 374-5p, and 20b-5p expression was changed by more than 2-fold between the post-caval lobectomy and corticosteroid administration groups.
Conclusions: Implanted fetal lung tissues established airway and capillary communication with the recipient lungs, and corticosteroids accelerated their maturation by promoting the differentiation of progenitor cells. The study findings provide new insights into lung regeneration research.

1. Introduction

The lung is an extremely difficult organ to regenerate as it is challenging to prepare a construction setup involving a large number of cells and promote cell differentiation and scaffold construction; it is also difficult to construct the lung in three dimensions [1–4]. Although extensive research has been conducted on lung regeneration, the development of functional organs has still not been achieved. With the rapid development of cell-based therapies using pluripotent stem cells, it may be possible to use a promising cell source to regenerate the alveolar region soon [5–11]. However, there is a dearth of fundamental understanding, and the

Abbreviations: ACE1, type I alveolar epithelial cells; ACE2, type II alveolar epithelial cells; BP, bipotential progenitor; DMEM, Dulbecco's modified Eagle's medium; MS, mechanical stretch; DEX, dexamethasone; H-E, Hematoxylin and eosin; SEM, scanning electron microscope; PBS, phosphate-buffered saline; CT, computed tomography; PDPN, podoplanin; SFTPC, surfactant protein C; CD, cluster of differentiation; miRNA, microRNA; FFPE, formalin fixed paraffin embedded; SD, standard deviation; ANOVA, analysis of variance; MSC, mesenchymal stem cell; EV, extracellular vesicle; BSA, bovine serum albumin.

* Corresponding author. Department of Thoracic and Endocrine Surgery and Oncology, Institute of Biomedical Sciences, University of Tokushima Graduate School, 3-18-15, Kuramotocho, Tokushima 770-8503, Japan.
E-mail address: ht1109@tokushima-u.ac.jp (H. Toba).

Peer review under responsibility of the Japanese Society for Regenerative Medicine.

https://doi.org/10.1016/j.reth.2023.09.006

clinical applicability may require some time. Moreover, as an alternative approach, we have attempted lung regeneration using the fetal rat lung tissue implantation model. In previous studies, we explored the characteristics of fetal rat lung tissue, which have great potential for further growth, differentiation, and proliferation, and used mesenchymal tissue as a suitable scaffold. The resulting implanted rat fetal lung tissues could survive and differentiate not only in normal rat adult lungs but also in diseased lungs (bleomycin-induced pulmonary fibrosis and emphysema) [12–14]. In addition, the graft mimicked the process of normal lung development and differentiation within the recipient lung based on the expression patterns of thyroid transcription factor-1 and Clara cell secretory protein [13]. However, we did not assess the functionality of the implanted fetal lung tissues.

The presence of cells that are progenitor cells of both type I alveolar epithelial cells (AEC1) and type II alveolar epithelial cells (AEC2) has been reported and are termed bipotential progenitor (BP) cells [15,16]. BP cells initially express molecular profiles of both ACE1 and ACE2 and differentiate by reducing the expression of other marker genes. BP cells may act as alveolar stem cells and play an important role in the regeneration of this region. However, the role of BP cells in the differentiation and maturation of the fetal lung has not yet been clarified.

The administration of corticosteroids in the late embryonic stage promotes the differentiation and maturation of fetal lungs [17,18]; this observation may be applied to implanted fetal rat lungs. The administration of corticosteroids may also promote the differentiation and maturation of implanted fetal lung tissue, and it may be possible to elucidate the mechanisms of engraftment and differentiation. Proving the existence of cells that play important roles in differentiation and maturation may contribute to the development of lung regenerative medicine.

This study aimed to evaluate the function of the implanted fetal lung tissue and investigate the mechanism of graft differentiation and maturation, focusing on alveolar stem cells.

2. Materials and methods

2.1. Animals

Specific pathogen-free male Lewis rats, aged approximately 8–12 weeks, were obtained from Charles River Laboratories Japan, Inc. (Kanagawa, Japan) and used as recipients. Pregnant rats at 17 days of gestation were obtained from Charles River Laboratories and mated with adult male Lewis rats for 1 d. Rats were maintained in an animal house on a layer of wood shavings in a pathogen-free environment, at an approximate temperature of 22 °C, under a 12-h light–dark cycle, and provided *ad libitum* access to water and food. All experiments were performed in accordance with the guidelines established by the Tokushima University Committee on Animal Care and Use. All the experimental protocols were reviewed and approved by the IACUC of Tokushima University, Japan (No. T2019-8).

2.2. Preparation of donors

Pregnant rats were euthanized under general anesthesia using an intraperitoneal injection of a mixture of medetomidine (0.375 mg/kg), midazolam (2 mg/kg), and butorphanol (2.5 mg/kg), and their fetuses were removed. The term of rat pregnancy is 22 days and can be divided into embryonic (before day 15) and subsequent fetal stages. From days 15–17, the fetal rat lung is in the pseudoglandular stage, which is followed by the canalicular (days 18 and 19) and saccular (days 20–22) stages [19]. In this study, fetal rat lung tissue at day 17 was used as a donor because this time point represents a pseudoglandular stage of vigorous differentiation and proliferation and is the earliest time allowing for lung removal through microscopic visualization. The fetal lungs were cut into fine pieces and stored in Dulbecco's modified Eagle's medium (DMEM) (Nacalai Tesque Ltd., Kyoto, Japan).

2.3. Implantation procedure

Fetal lung grafts were implanted as described in our previous study [12]. Briefly, adult rats were subcutaneously administered atropine sulfate at 0.1 mg/body and butorphanol tartrate at 1 mg/body and ventilated with a small animal respirator (SN480-7, Shinano Ltd, Tokyo, Japan) at 70 cycles/min, a tidal volume of 10 mL/kg, and a positive end-expiratory pressure of 2 cm H_2O under 2% isoflurane. The study involved three treatment groups. For group 1 (mechanical stretch- [MS-] group, n = 19), after left thoracotomy, 0.1 mL DMEM-containing lung fragments from two fetuses were injected just under the pleura of the left lung apex using a 0.25-mL syringe and 20-gauge peripheral venous catheter. The left lung was ligated and resected at the level of the pulmonary vein. In group 2 (MS + group, n = 22), after injecting the fetal lung grafts, the left lung under the level of the pulmonary vein was ligated and resected, and the postcaval lobe was resected by opening the mediastinal pleura, to avoid shifting to the left thoracic cavity. Group 3 (dexamethasone [DEX] group, n = 24) was subjected to the same surgical procedure as group 2, following which dexamethasone (1 mg/kg) was injected intramuscularly for seven consecutive days from the day of surgery. The animals (4–6 per group) were euthanized 3 days and 1, 2, and 4 weeks after implantation.

2.4. Histology

The lungs were perfused with saline through the pulmonary artery after cutting the left atrium, removed en bloc with the heart, and fixed using fixing solution (4% paraformaldehyde: optimal cutting temperature (OCT) compound = 4:1) from the trachea at 15 cm H_2O. Specimens embedded in paraffin were cut at 5-μm thickness and stained with hematoxylin and eosin (H-E) or used for immunofluorescence analysis. Light microscopy images of histological specimens were captured using a microscope BZ-X800 (Keyence Ltd., Osaka, Japan).

To quantify the implanted fetal lung expansion, the alveolar space was measured semi-automatically using software (BZ-H4C/Hybrid Cell Count, Keyence Ltd). At 400× magnification, using a light microscope, five fields were randomly selected from each implanted fetal lung, and the measurement conditions were set to extract only the ``air'' part to avoid including the lung parenchyma, such as the alveolar septum. The proportion of the alveolar (air) space in the images was measured.

2.5. Scanning electron microscopy

The specimens were fixed with 8% neutral formalin adjusted to pH 7.4 at 4 °C for 24 h, washed several times with phosphate-buffered saline (PBS), fixed at 4 °C for 24 h, and fixed with 2.5% glutaraldehyde at 4 °C for 24 h. The alveolar and capillary vessels in the graft were observed, focusing on fusion of the normal and implanted lungs. Sections were imaged using an S-800 scanning electron microscope (SEM; Hitachi Ltd., Tokyo, Japan).

2.6. Computed tomography

To objectively evaluate changes in the grafts over time, micro-computed tomography (CT) scans (LaTheta LCT-200; Hitachi Ltd) were performed on the same animals. The animals were sedated

with 2% isoflurane and examined in the prone position. The grafts were evaluated by measuring the CT value of the slice with the largest graft diameter. The graft in the CT image was manually surrounded, structures with CT values in the range of −200 to 200 were extracted, and the mean values were measured. Four animals in each group were examined at 7, 14, 28, and 56 days after implantation.

2.7. Immunofluorescence

To identify BP cells in implanted grafts and observe their differentiation over time, we performed immunofluorescence staining with *anti*-podoplanin (PDPN) antibody for AEC1 and anti-surfactant protein C (SFTPC) antibody for AEC2. In addition, we examined a cluster of differentiation (CD) 31 staining to assess interstitial blood flow. Paraffin-embedded sections were deparaffinized, and antigens were retrieved using the 2100 Antigen Retriever (Aptum Biologics Ltd., Southampton, UK) containing antigen retrieval solution at pH 9 (415,201; Nichirei Ltd.) for 2.5 h. The sections were blocked using 5% bovine serum albumin (BSA)/PBS containing 10% donkey serum for 2 h at 15–25 °C and the following directly conjugated antibodies (1:100 in 5% BSA/PBS) were then used for labeling: anti-mouse PDPN antibody conjugated with Alexa Fluor® 488 (NB110-96423 AF488; Novus Biologicals, Englewood, Co, USA), anti-mouse SFTPC antibody conjugated to Alexa Fluor 594 (sc-518,029 AF594; Santa Cruz Biotechnologies, Santa Cruz, CA, USA), and anti-rabbit CD31 antibody-conjugated Alexa Fluor 647 (bs-0468R-A647; Bioss, Worbun, MA, USA). After incubation with the antibodies for 2 h at room temperature in a shaded humidification chamber, the sections were washed thrice with PBS/0.3% Triton X and twice in PBS. The sections were incubated with an autofluorescent inhibitor (SP-8400; Vector Laboratories, Newark, CA, USA), washed once with PBS, and mounted with DAPI (H-1800; Vector Laboratories.). Immunostaining fluorescence was observed, and images were captured using a fluorescence microscope BZ-X800 (Keyence).

Specimens collected on 7 and 14 days after surgery were evaluated by counting the number of BP cells. Immunofluorescence images of the implanted grafts were captured, five images were randomly selected, and cells positive for both PDPN and SFTPC were counted manually.

2.8. RNA extraction and microRNA (miRNA) expression profiling

Formalin-fixed paraffin-embedded (FFPE) samples from each group were analyzed on day 7. Four animals were used per group; 30 sections (10-μm) were prepared from each FFPE specimen and RNA was extracted. The extracted RNA was processed using a silica-based spin column (Toray Industries Inc., Tokyo, Japan) to obtain purified total RNA. The degree of RNA crosslinking and degradation was analyzed via electrophoresis using an Agilent 2100 Bioanalyzer (Agilent Technologies, Santa Clara, CA, USA).

The extracted total RNA was labeled using a 3D-Gene miRNA labeling Kit (Toray Industries Inc.). The labeled RNAs were hybridized onto a 3D-Gene Rat miRNA Oligo chip (Toray Industries Inc.). After stringent washes, fluorescent signals were scanned using a 3D-Gene Scanner (Toray Industries Inc.) and analyzed using 3D-Gene Extraction software (Toray Industries Inc.). Among the examined miRNAs, those with one blank value in the four samples were excluded because of noise.

2.9. Statistical analyses

All analyses were conducted using the SPSS software (version 27, IBM Corp., Armonk, NY, USA). All statistical tests were two-sided, and $p < 0.05$ was considered significant. All continuous values are expressed as means ± standard error. Alveolar areas were compared using a two-way analysis of variance (ANOVA), and multiple comparisons among groups were performed using Tukey's test. CT values were compared using one-way ANOVA with repeated measurements, and multiple comparisons between groups were evaluated using Tukey's test. BP cell numbers were compared using the Kruskal–Wallis method. The increase in α error due to multiple comparisons among groups was adjusted using Bonferroni correction (p-value tripled).

3. Results

3.1. Formation of alveolar spaces in the graft confirms the establishment of airway and capillary networks

The implanted fetal lung tissues survived and differentiated on day 28, similar to the findings of our previous study [12,13] (Fig. 1A). Numerous alveolar spaces were formed within the graft, and immunostaining of the donor lung and graft revealed that the alveoli were composed of ACE1 and ACE2 (Fig. 1B). Immunostaining revealed PDPN expression around the alveolar space, and the staining intensity increased as the space expanded. Additionally, SFTPC-positive cells were observed at high graft densities. SEM analysis of the microstructure revealed multiple alveolar pores formed between the donor lung and graft (Fig. 1C). CD31 was expressed in the interstitial tissue in contact with the PDPN-positive cells, indicating the formation of a capillary network (Fig. 1D).

3.2. Mechanical stretch and steroids further expand alveolar spaces

H-E staining showed time-based expansion of the implanted fetal lung tissues and alveoli formation in each group (Fig. 2A–L). The grafts appeared to be similar in each group on day 3, but after day 7, the alveolar space expanded well in the order of DEX group > MS + group > MS- group at the same time point. A comparison of the automatically measured alveolar space areas showed significant differences among the groups and time points, and multiple comparisons showed that the alveolar space in the DEX group was the largest (Fig. 2M).

CT images identified the grafts; however, the borders of the donor lung were initially unclear. The borders between the graft and donor lung clarified with time, and the density of the graft became more pneumatic and vaguer (Fig. 3A–L). The mean CT values decreased over time, reflecting improved air content within the graft and aligning with both the vague change in CT and the enlargement of the alveolar space in the microscopic findings (Fig. 3M). The mean CT values of the DEX and MS + groups decreased gradually over time compared to those of the MS + group, with a statistically significant difference between the MS- group and DEX group ($p = 0.034$). This may indicate air space expansion of the grafts, consistent with the histological findings (Fig. 2A–L). However, the graft showed limited air presence on CT, even in the DEX group. In our previous study [12], we followed up to 12 weeks after implantation and histologically confirmed considerably wider alveolar space. Therefore, a longer follow-up would have enabled a clearer observation of the air density area.

3.3. Corticosteroids accelerate the maturation of BP cells into alveolar epithelial cells

The number of BP (PDPN+/SFTPC+) cells in the grafts was counted. Numerous SFTPC-positive cells were found in the graft, some of which were co-positive for PDPN, which were recognized

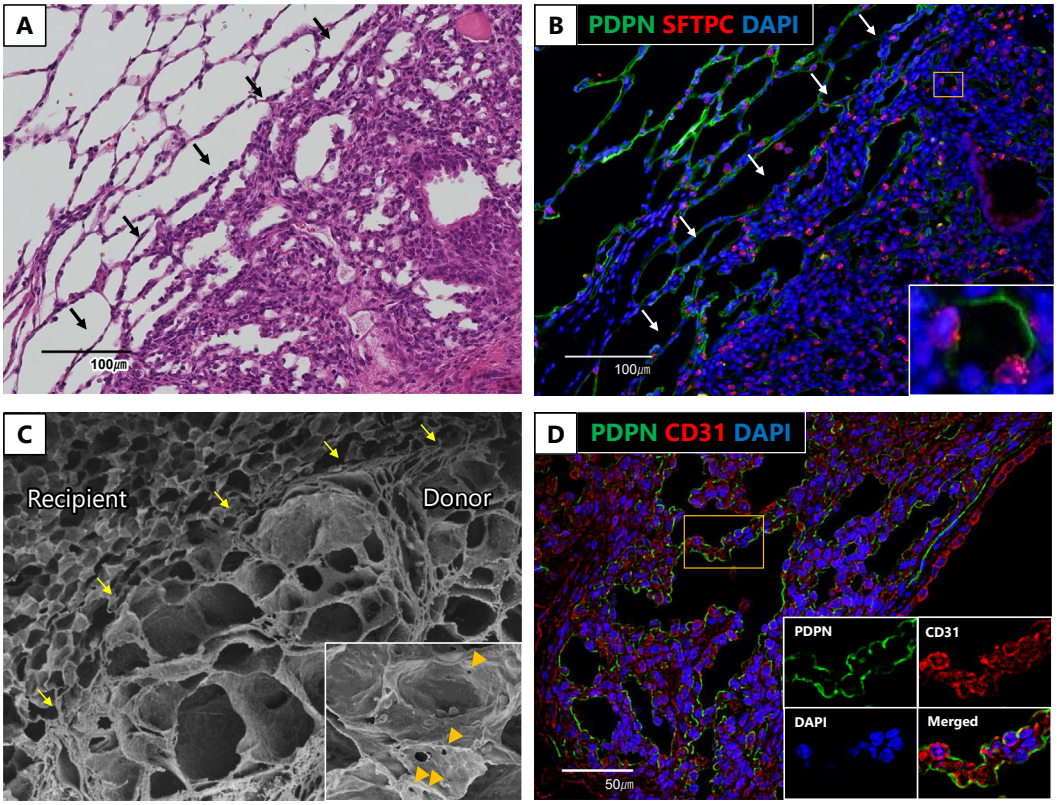

Fig. 1. The graft at 28 days after implantation. Alveolar spaces were formed in the graft, which confirmed the establishment of airway and capillary networks. (A) Microscopic image of hematoxylin and eosin (H–E) staining. There is no apparent immune response in the graft and recipient lungs. Numerous alveolar spaces were formed within the graft, arrow = boundary between donor and recipient. (B) Immunohistochemical staining for podoplanin (PDPN) and surfactant protein C (SFTPC). Similar immunostainability of donor lung and graft was observed, and the alveoli were composed of type I alveolar epithelial cells (PDPN+) and type II alveolar epithelial cells (SFTPC+). SFTPC + cells were observed at high density in the graft, arrow = Boundary between donor and recipient tissue. (C) Scanning electron microscopy results. Multiple alveolar pores formed between the donor lung and the graft, arrow = boundary between donor and recipient, arrow-head = alveolar pores. (D) Immunohistochemical staining for a cluster of differentiation (CD) 31 and PDPN. CD31 was expressed in the interstitial tissue in contact with PDPN + cells.

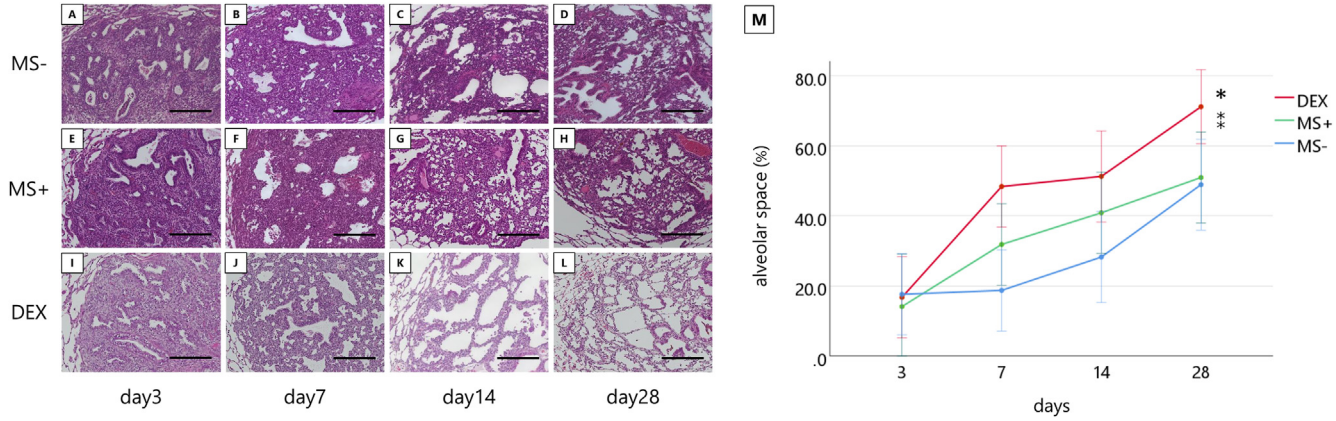

Fig. 2. Time-dependent changes in grafts observed with hematoxylin and eosin (H–E) staining and comparison of alveolar spaces among the three groups. (A–L) H-E staining images. Time-dependent expansion of the alveolar spaces was observed in all the groups but was particularly remarkable in the dexamethasone (DEX) group. (I–L) The differences were not remarkable on day 3 but were distinct on day 14 or day 28, bar = 100μm. (M) comparison of semi-automatically measured alveolar spaces among the three groups. Alveolar spaces showed significant differences among the groups and time points, and multiple comparisons showed that the alveolar space of the DEX group was the largest. Statistical comparisons were performed using two-way analysis of variance (ANOVA) and multiple comparisons with Tukey's test.*p = 0.020, compared to the mechanical stretch(MS) + group, ⁑p < 0.001, compared to the MS- group, Error bar = ± 2 standard error.

as BP cells (Fig. 4A–C). In these cells, the cytoplasm was stained with SFTPC, and PDPN was expressed on the cell membrane surrounding the cells (Fig. 4D). BP cells were localized in contact with the alveolar space or present in a group of cells that were about to expand and form alveolar spaces. On day 7, BP cell numbers of the DEX group were significantly lower than those of the MS- group ($p = 0.032$) and tended to be insignificantly lower than those of the MS + group ($p = 0.093$) (Fig. 4E). However, on day 14, the BP numbers were almost the same among the three groups, indicating that corticosteroids could accelerate graft maturation by regulating the differentiation of BP cells at an early stage after implantation.

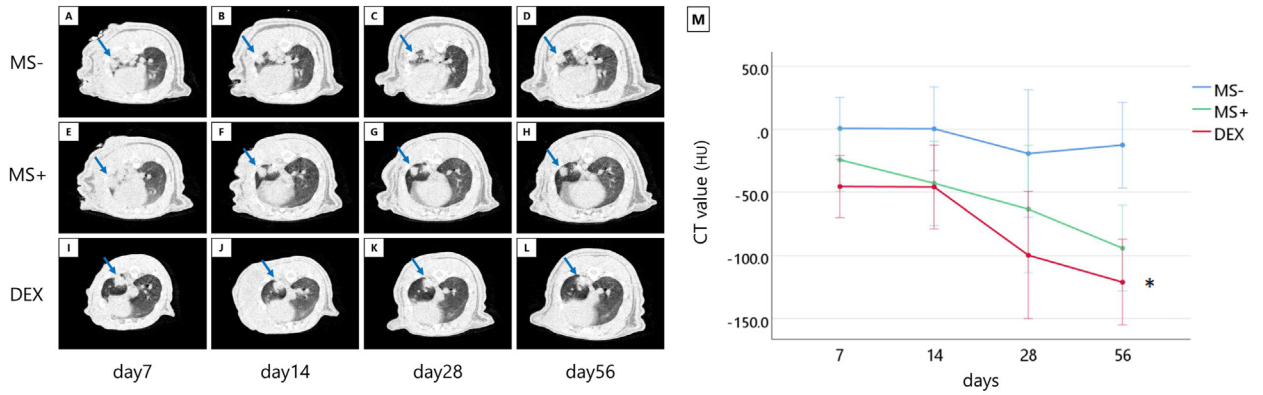

Fig. 3. Time-dependent changes in grafts using computed tomography (CT) images and comparison of CT values among the three groups. (A–L) CT images displayed the grafts, but the borders with the donor lung were initially unclear. The borders between the graft and the donor lung became clear with time, and the density of the graft became more pneumatic and vaguer. arrow = the implanted grafts. (M) Comparison of the CT values of the grafts among the three groups. One-way ANOVA with repeated measurements showed a time-dependent decrease in CT values, and multiple comparisons using Tukey's test showed a significant difference between the dexamethasone (DEX) group and the mechanical stretch (MS)- group.*p = 0.034, Error bar = ± 2 standard error.

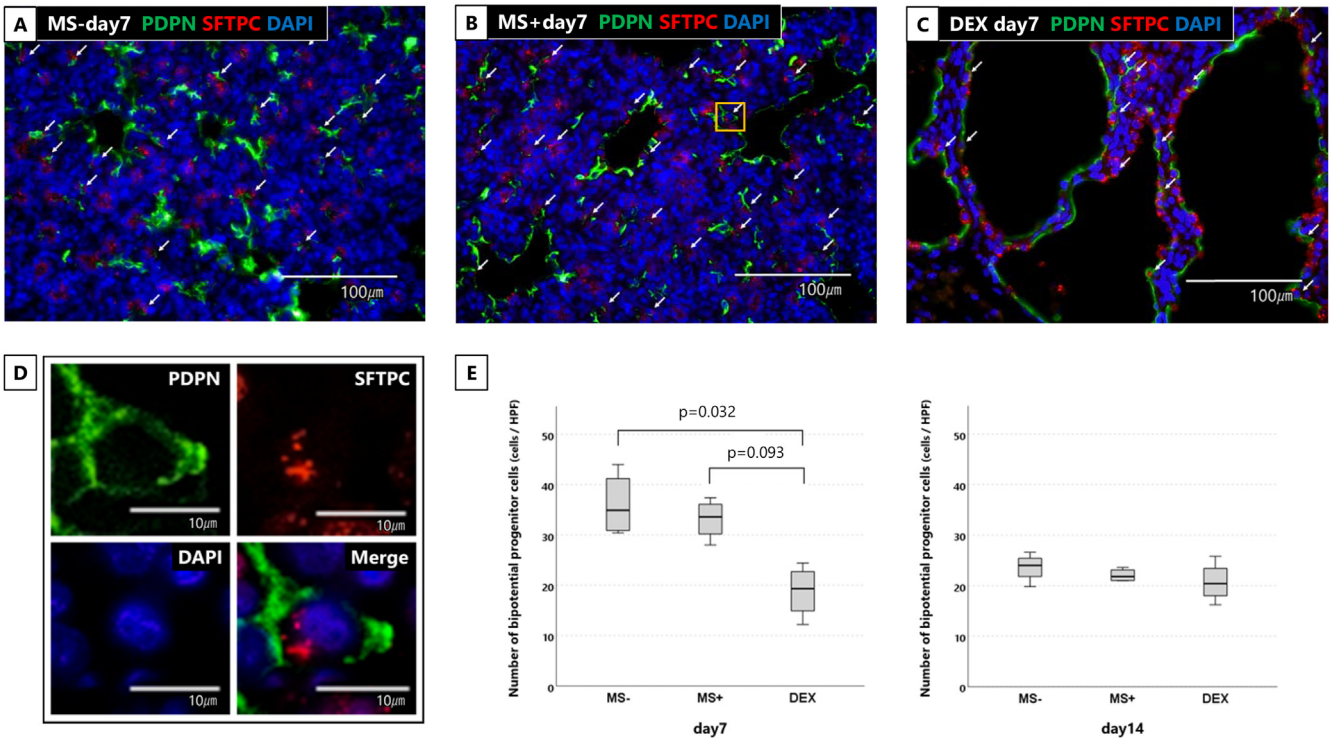

Fig. 4. Immunohistochemical staining for podoplanin (PDPN) and surfactant protein C (SFTPC) of the graft at 7 days after implantation. Some SFTPC + cells also expressed PDPN. These cells were considered as bipotential progenitor (BP) cells, and BP cell number was determined and compared. (A) PDPN and SFTPC co-staining image, 7 days after implantation in the mechanical stretch (MS)- group. Formation of the alveolar space is still inadequate, with a particularly large number of PDPN + /SFTPC + cells (BP cells) present in the unexpanded area of the graft. Arrow = BP cells. (B) PDPN and SFTPC co-staining image, 7 days after implantation in the MS + group. Similar to the MS- group, a large number of BP cells were observed in the unexpanded area of the graft. arrow = BP cells. (C) PDPN and SFTPC co-staining image, 7 days after implantation in the dexamethasone (DEX) group. Due to the formation of the alveolar spaces by graft differentiation, few BP cells should be present in the parenchyma. arrow = BP cells. (D) Magnified image of the BP cells in Figure B. The cytoplasm was stained with SFTPC, and PDPN was expressed on the cell membrane surrounding the cells. (E) Comparative quantification of BP cells among the three groups, 7 and 14 days after implantation. BP cell number was significantly lower in the DEX group, 7 days after implantation, but there was no difference on the 14th day. Statistical comparisons were performed using the Kruskal–Wallis method and multiple comparisons among the groups were adjusted using Bonferroni correction.*p = 0.032, ‡p = 0.093, HPF, high power field = 362.34 × 271.76 μm.

3.4. Expression of miRNAs in grafts is altered by the effects of corticosteroids

To determine the role of corticosteroids in the differentiation of BP toward the maturation of the grafts, miRNA expression was comprehensively compared among the three groups using samples from day 7 after implantation. The detected miRNAs were clustered and are shown in a heatmap (Fig. 5). We extracted corticosteroid-affected miRNAs (fold-change >1.50 or fold-change <0.67), including eight upregulated and 19 downregulated miRNAs (Table 1). In addition, three miRNAs that met the more stringent criteria (fold-change> 2.0 or fold-change <0.50) were extracted: upregulated 487b-3p and downregulated 374-5p and 20b-5p.

4. Discussion

Our previous studies have revealed that implanted fetal rat lung fragments can survive and differentiate between normal and diseased lungs [12–14]. In addition, we have also shown that the re-establishment of blood perfusion in the grafts occurs by injecting Indian ink into the recipients' pulmonary arteries [12] and that implanted fetal lung tissues in the recipients followed the differentiation process of normal lungs, evidenced by the results of immunostaining with CCSP and TTF-1 [13]. Although we also showed, using H-E staining, that the grafts in the recipients could morphologically form alveolus-like structures, functional lungs require that airflow exists in the formed alveoli and blood flow exists in the formed capillary networks [3]. In this study, the graft developed an alveolar structure composed of ACE1 and ACE2 on day 28 and the interstitium had CD31-positive capillary networks. Furthermore, ultrastructural observations revealed that the graft and recipient cells communicated through the alveolar pores. These findings indicate that the grafts could differentiate and mature into normal alveoli, enabling gas exchange in the lungs. Notably, fetal lung tissues could not survive and differentiate when implanted into the omentum and subcutaneously. In addition, even when adult lung tissues were implanted as grafts, they exhibited fibrotic changes and could not survive unlike fetal lung tissues in our previous study [12]. These results suggest that the phenomena of implanted fetal lung tissues observed only in the adult lung were tissue-specific. Therefore, owing to the unique properties of fetal lung tissue, we believe that the grafts could establish a connection with the recipients, resulting in the formation of new alveolar pores. However, further experiments investigating the detailed mechanisms are required.

Grafts might follow the normal fetal rat lung morphogenetic course in the recipient lung as part of the mechanism of differentiation [13]. In the present study, we discovered a new potential mechanism of graft differentiation and maturation using a corticosteroid-administered model. We focused on corticosteroids because they are widely known to promote fetal lung differentiation and are clinically used in human and mouse experimental models [17,18,20]. Moreover, mechanical stretch is known to promote alveolarization [12,21]. In this study, alveolar spaces tended to expand more in the MS + group than in the MS- group, although the difference was statistically insignificant. In contrast, the administration of DEX evidently promoted the expansion of alveolar spaces. BP cells exist as local progenitor cells in normal fetal lungs and play a role in alveolar differentiation and maturation [15,16,21]. Immunostaining results revealed the presence of many local stem cells in a cellular state before branching. During the pre-sacculation period of the fetal lung, many BP cells are known to be present in the part that develops into the alveoli [15,16]. As sacculation progresses from the proximal side, BP cells differentiate into ACE1 or ACE2, and the number of BP cells decreases during differentiation and the maturation of the fetal lung. In this study, the number of BP cells in the DEX group decreased significantly with an expansion of the alveolar space on day 7, but the significant difference disappeared on day 14. Based on this result, we speculated that steroids affected the time at which the alveolar spaces began to expand, inducing the differentiation of local stem cells and promoting graft maturation. This result also indicates the importance of BP in graft differentiation and maturation.

To further explore these findings, we focused on graft-secreted miRNAs and evaluated them using microarrays. To test whether

Table 1
Differential miRNA expression among three groups.

Name	Log 2 (75th percentile normalization)			ratio (DEX/MS+)
	MS-	MS+	DEX	
rno-miR-487b-3p	0.612	0.399	1.402	2.003
rno-miR-125b-1-3p	−0.253	0.557	1.422	1.821
rno-miR-223-3p	3.104	3.059	3.796	1.667
rno-miR-22-5p	−0.355	−0.505	0.162	1.588
rno-miR-21-5p	5.212	5.103	5.753	1.569
rno-miR-532-3p	−0.877	−0.293	0.311	1.521
rno-miR-133b-3p	0.943	0.709	1.310	1.517
rno-miR-451-5p	2.084	2.062	2.656	1.510
rno-miR-128-3p	−1.010	0.159	−0.428	0.666
rno-miR-503-5p	0.977	0.883	0.291	0.664
rno-miR-423-3p	−0.326	−0.131	−0.727	0.661
rno-miR-129-2-3p	−0.674	−0.463	−1.070	0.656
rno-miR-1949	1.128	1.178	0.562	0.652
rno-miR-299a-3p	−1.384	−0.791	−1.429	0.643
rno-miR-106b-3p	−0.850	−0.147	−0.789	0.641
rno-miR-292-5p	−0.319	−0.092	−0.736	0.640
rno-let-7i-3p	−0.745	−0.263	−0.941	0.625
rno-miR-146a-5p	2.654	2.820	2.136	0.623
rno-miR-330-3p	−1.730	−0.397	−1.092	0.618
rno-miR-342-3p	0.063	0.180	−0.534	0.610
rno-miR-218a-5p	1.418	1.358	0.624	0.601
rno-miR-204-5p	−0.309	0.114	−0.656	0.587
rno-miR-205	0.478	0.593	−0.218	0.570
rno-miR-10a-3p	−1.176	−0.649	−1.475	0.564
rno-miR-331-3p	−0.386	0.058	−0.855	0.531
rno-miR-374-5p	−0.392	−0.318	−1.434	0.461
rno-miR-20b-5p	2.137	2.233	0.972	0.417

rno-miR: *Rattus norvegicus* microRNA, MS-; Mechanical stretch-group, MS+; Mechanical stretch + group, DEX: dexamethasone-administered group.
List of miRNAs whose expression levels changed due to the effects of corticosteroids. The miRNAs were filtered with a fold-change> 1.50 or fold-change <0.67, and 8 upregulated and 19 downregulated genes were detected.

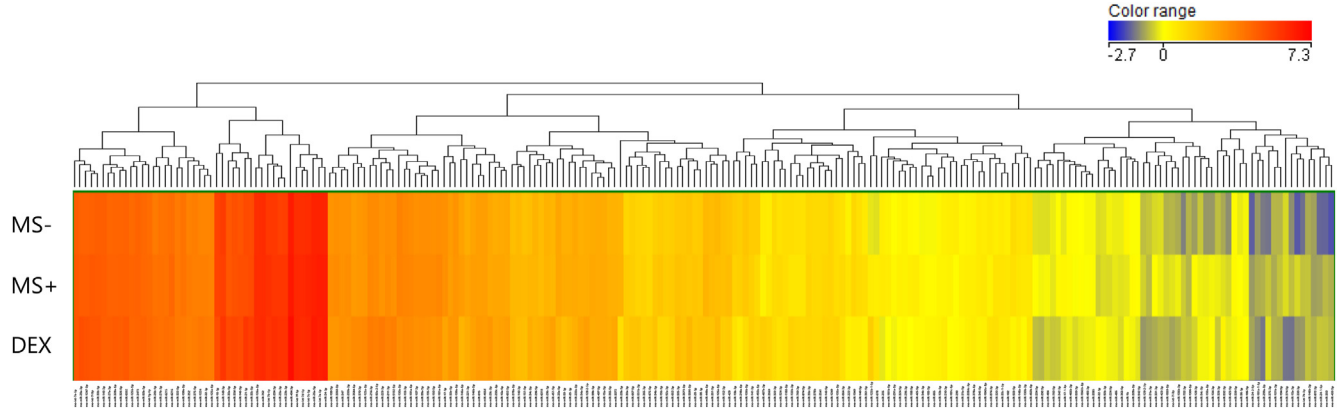

Fig. 5. A heat map comparing miRNA expression on day 7 after implantation in the mechanical stretch (MS)-, MS+ and dexamethasone (DEX) groups. We measured four samples in each group; miRNAs with blank values were excluded as noise. The 222 genes extracted were clustered as shown.

corticosteroids affect grafts, some miRNAs were extracted. Some of the differentially expressed miRNAs, such as let-7, miRNA-125, and miRNA-21, were associated with normal lung development [22], which is consistent with previous reports. Furthermore, we identified three new miRNAs (miRNA-487b-3p, miRNA-20b-5p, and miRNA-374-5p) which showed significant changes in fold-change >2.0, fold-change <0.5 or more in steroid-administered models. These miRNAs have not yet been reported to be involved in lung development or differentiation of lung progenitor cells. MiRNA-487b-3p is a member of the miRNA-154 family and plays an important role in cell growth, proliferation, and differentiation [23]. In addition, upregulated miRNA-487b can enhance the proliferation, migration, and invasion of human endothelial cells, consequently contributing to angiogenesis [24]. MiRNA-487b is highly expressed in fetal lungs [25]. Therefore, miRNA-487b-3p may be involved in fetal lung maturation through cell differentiation and angiogenesis. MiRNA-20b-5p is a member of the miRNA-17 gene family, and its downregulation suppresses the stemness of cancer stem cells, consequently promoting their differentiation in colorectal cancer [26] and regulating the phenotype of mesenchymal stem cells via the endothelial PAS domain 1 transcription factor [27]. MiRNA-374-5p is a member of the miRNA-374 family which contributes to the differentiation and proliferation of different cells in multiple organisms [28]; however, there are no reports of its relationship with stem cell differentiation. Nevertheless, miRNAs are known to be the prime candidates for mediating the regenerative effects observed on lung development [29]. Therefore, corticosteroids may have promoted BP cell differentiation, which in turn promoted differentiation and maturation of the implanted fetal lungs by involving miRNAs, including those mentioned above.

Cell-based lung regenerative medicine may exhibit paracrine properties by replacing damaged stem cells or by administering miRNAs derived from stem cells with extracellular vesicles (EV) [30–32]. Transbronchial administration of stem cells or organoids has been developed as a replacement for damaged stem cells [9,33]. Because the selection of cells to be administered is an important factor in this method, it was useful to show the existence of local stem cells and the mechanism of differentiation in this study. Moreover, EV treatments with miRNA as cargo have also been reported [34,35]. The miRNAs identified in this study may serve as potential candidates for such treatments. In addition, our finding that corticosteroids may regulate these miRNAs to promote BP cell differentiation and accelerate graft maturation is insightful. We hope that the findings of this study will lead to the development of regenerative medicine and treatments for lung diseases in premature infants.

A limitation of this study is that it only demonstrated that the airway and blood flow of the graft are connected, and functional evaluation was not performed. In addition, the long-term side effects of steroids have not been considered. Furthermore, it has not been revealed whether the miRNAs of interest play a role in stem cell differentiation; therefore, further research is required. Nevertheless, the discovery of new miRNAs involved in lung development and progenitor cell differentiation is important and will provide new insights into the field. The miRNA expression profiles during lung development in humans and mice are similar [36], and this result may be applicable to humans. Finally, in addition to these academic issues, there are ethical concerns regarding the use of fetal tissue for treatment.

We expect that the study findings will be applicable to the treatment of induced stem cells, which may have potential for clinical treatment.

5. Conclusions

Implanted fetal lung tissues formed airway and capillary communications with the recipient lungs, and corticosteroids accelerated their maturation by promoting the differentiation of progenitor cells by regulating some miRNAs. The study findings provide new insights into lung regeneration research.

Funding

This study was supported by the Japan Society for the Promotion of Science, KAKENHI (grant number 17K16609).

IRB number

IACUC of the Tokushima University, Japan (No. T2019-8).

Declaration of competing interest

None declared.

Appendix A. Supplementary data

Supplementary data related to this article can be found at https://doi.org/10.1016/j.reth.2023.09.006.

References

[1] Nichols JE, Cortiella J. Engineering of a complex organ: progress toward development of a tissue-engineered lung. Proc Am Thorac Soc 2008;5:723–30.
[2] Hogan BL, Barkauskas CE, Chapman HA, Epstein JA, Jain R, Hsia CC, et al. Repair and regeneration of the respiratory system: complexity, plasticity, and mechanisms of lung stem cell function. Cell Stem Cell 2014;15:123–38.
[3] Dorrello NV, Guenthart BA, O'Neill JD, Kim J, Cunningham K, Chen YW, et al. Functional vascularized lung grafts for lung bioengineering. Sci Adv 2017;3:e1700521.
[4] Basil MC, Katzen J, Engler AE, Guo M, Herriges MJ, Kathiriya JJ, et al. The cellular and physiological basis for lung repair and regeneration: past, present, and future. Cell Stem Cell 2020;26:482–502.
[5] Huang SX, Islam MN, O'Neill J, Hu Z, Yang YG, Chen YW, et al. Efficient generation of lung and airway epithelial cells from human pluripotent stem cells. Nat Biotechnol 2014;32:84–91.
[6] Gotoh S, Ito I, Nagasaki T, Yamamoto Y, Konishi S, Korogi Y, et al. Generation of alveolar epithelial spheroids via isolated progenitor cells from human pluripotent stem cells. Stem Cell Rep 2014;3:394–403.
[7] Yamamoto Y, Gotoh S, Korogi Y, Seki M, Konishi S, Ikeo S, et al. Long-term expansion of alveolar stem cells derived from human iPS cells in organoids. Nat Methods 2017;14:1097–106.
[8] Miller AJ, Hill DR, Nagy MS, Aoki Y, Dye BR, Chin AM, et al. In vitro induction and in vivo engraftment of lung bud tip progenitor cells derived from human pluripotent stem cells. Stem Cell Rep 2018;10:101–19.
[9] Ikeo S, Yamamoto Y, Ikeda K, Sone N, Korogi Y, Tomiyama L, et al. Core-shell hydrogel microfiber-expanded pluripotent stem cell-derived lung progenitors applicable to lung reconstruction in vivo. Biomaterials 2021;276:121031.
[10] Ghaedi M, Calle EA, Mendez JJ, Gard AL, Balestrini J, Booth A, et al. Human iPS cell-derived alveolar epithelium repopulates lung extracellular matrix. J Clin Invest 2013;123:4950–62.
[11] Konishi S, Gotoh S, Tateishi K, Yamamoto Y, Korogi Y, Nagasaki T, et al. Directed induction of functional multi-ciliated cells in proximal airway epithelial spheroids from human pluripotent stem cells. Stem Cell Rep 2016;6:18–25.
[12] Kenzaki K, Sakiyama S, Kondo K, Yoshida M, Kawakami Y, Takehisa M, et al. Lung regeneration: implantation of fetal rat lung fragments into adult rat lung parenchyma. J Thorac Cardiovasc Surg 2006;131:1148–53.
[13] Toba H, Sakiyama S, Kenzaki K, Kawakami Y, Uyama K, Bando Y, et al. Implantation of fetal rat lung fragments into bleomycin-induced pulmonary fibrosis. J Thorac Cardiovasc Surg 2012;143:1429–35.
[14] Uyama K, Sakiyama S, Yoshida M, Kenzaki K, Toba H, Kawakami Y, et al. Lung regeneration by fetal lung tissue implantation in a mouse pulmonary emphysema model. J Med Invest 2016;63:182–6.
[15] Desai TJ, Brownfield DG, Krasnow MA. Alveolar progenitor and stem cells in lung development, renewal and cancer. Nature 2014;507:190–4.
[16] Treutlein B, Brownfield DG, Wu AR, Neff NF, Mantalas GL, Espinoza FH, et al. Reconstructing lineage hierarchies of the distal lung epithelium using single-cell RNA-seq. Nature 2014;509:371–5.
[17] McGoldrick E, Stewart F, Parker R, Dalziel SR. Antenatal corticosteroids for accelerating fetal lung maturation for women at risk of preterm birth. Cochrane Database Syst Rev 2020;25:CD004454.
[18] Gilstrap LC, Christensen R, Clewell WH, D'Alton ME, Davidson Jr EC, Escobedo MB, et al. Effect of corticosteroids for fetal maturation on

perinatal outcomes: nih consensus development panel on the effect of corticosteroids for fetal maturation on perinatal outcomes. JAMA 1995;273:413–8.
[19] Schittny JC. Development of lung. Cell Tissue Res 2017;367:427–44.
[20] Yu HR, Li SC, Tseng WN, Tain YL, Chen CC, Sheen JM, et al. Early and late effects of prenatal corticosteroid treatment on the microRNA profiles of lung tissue in rats. Exp Ther Med 2016;11:753–62.
[21] Nguyen TM, Merwe Jvd, Rendin LE, Larsson-Callerfelt A-K, Deprest J, Westergren-Thorsson G, et al. Stretch increases alveolar type 1 cell number in fetal lungs through ROCK-Yap/Taz pathway. Am J Physiol Lung Cell Mol Physiol 2021;321:L814–26.
[22] Lu Y, Okubo T, Rawlins E, Hogan BL. Epithelial progenitor cells of the embryonic lung and the role of microRNAs in their proliferation. Proc Am Thorac Soc 2008;5:300–4.
[23] Yi H, Geng L, Black A, Talmon G, Berim L, Wang J. The miR-487b-3p/GRM3/TGFβ signaling axis is an important regulator of colon cancer tumorigenesis. Oncogene 2017;36:3477–89.
[24] Feng N, Wang Z, Zhang Z, He X, Wang C, Zhang L. miR-487b promotes human umbilical vein endothelial cell proliferation, migration, invasion and tube formation through regulating THBS1. Neurosci Lett 2015;591:1–7.
[25] Milosevic J, Pandit K, Magister M, Rabinovich E, Ellwanger DC, Yu G, et al. Profibrotic role of miR-154 in pulmonary fibrosis. Am J Respir Cell Mol Biol 2012;47:879–87.
[26] Tang D, Yang Z, Long F, Luo L, Yang B, Zhu R, et al. Long noncoding RNA MALAT1 mediates stem cell-like properties in human colorectal cancer cells by regulating miR-20b-5p/Oct 4 axis. J Cell Physiol 2019;234:20816–28.
[27] Giraud-Triboult K, Rochon-Beaucourt C, Nissan X, Champon B, Aubert S, Piétu G. Combined mRNA and microRNA profiling reveals that miR-148a and miR-20b control human mesenchymal stem cell phenotype via EPAS1. Physiol Genom 2011;43:77–86.
[28] Bian H, Zhou Y, Zhou D, Zhang Y, Shang D, Qi J. The latest progress on miR-374 and its functional implications in physiological and pathological processes. J Cell Mol Med 2019;23:3063–76.
[29] Antounians L, Catania VD, Montalva L, Liu BD, Hou H, Chan C, et al. Fetal lung underdevelopment is rescued by administration of amniotic fluid stem cell extracellular vesicles in rodents. Sci Transl Med 2021;13:eaax5941.
[30] Lu Q, El-Hashash AHK. Cell-based therapy for idiopathic pulmonary fibrosis. Stem Cell Invest 2019;6:22.
[31] Mohan A, Agarwal S, Clauss M, Britt NS, Dhillon NK. Extracellular vesicles: novel communicators in lung diseases. Respir Res 2020;21:175.
[32] Khalaj K, Figueira RL, Antounians L, Lauriti G, Zani A. Systematic review of extracellular vesicle-based treatments for lung injury: are EVs a potential therapy for COVID-19? J Extracell Vesicles 2020;9:1795365.
[33] Alvarez-Palomo B, Sanchez-Lopez LI, Moodley Y, Edel MJ, Serrano-Mollar A. Induced pluripotent stem cell-derived lung alveolar epithelial type II cells reduce damage in bleomycin-induced lung fibrosis. Stem Cell Res Ther 2020;11:213.
[34] Aliotta JM, Pereira M, Wen S, Dooner MS, Del Tatto M, Papa E, et al. Exosomes induce and reverse monocrotaline-induced pulmonary hypertension in mice. Cardiovasc Res 2016;110:319–30.
[35] Fang SB, Zhang HY, Wang C, He BX, Liu XQ, Meng XC, et al. Small extracellular vesicles derived from human mesenchymal stromal cells prevent group 2 innate lymphoid cell-dominant allergic airway inflammation through delivery of miR-146a-5p. J Extracell Vesicles 2020;9:1723260.
[36] Williams AE, Moschos SA, Perry MM, Barnes PJ, Lindsay MA. Maternally imprinted microRNAs are differentially expressed during mouse and human lung development. Dev Dynam 2007;236:572–80.